Large-scale simulations of ballistic deposition: The approach to asymptotic scaling

Bahman Farnudi
Institute for Advanced Studies in Basic Sciences (IASBS), Zanjan 45137-66731, Iran

Dimitri D. Vvedensky
The Blackett Laboratory, Imperial College London, London SW7 2AZ, United Kingdom

(Dated: December 20, 2010)

Extensive kinetic Monte Carlo simulations are presented for ballistic deposition (BD) in $(1+1)$ dimensions. Asymptotic scaling is found only for lattice sizes $L \gtrapprox 2^{12}$. Such a large system size for the onset of scaling explains the widespread discrepancies of previous reports for exponents of BD in one and likely higher dimensions. The exponents obtained from our simulations, $\alpha = 0.499 \pm 0.004$ and $\beta = 0.336 \pm 0.004$, are in excellent agreement with the exact values $\alpha = \frac{1}{2}$ and $\beta = \frac{1}{3}$ for the one-dimensional Kardar–Parisi–Zhang equation. Our findings enable a more informed exploration of exponents for BD in higher dimensions, accurate estimates of which have proven to be elusive.

PACS numbers: 05.40.-a, 81.15.Aa, 05.10.Gg

Fluctuations of growing surfaces are often described by idealized models [1–3] wherein the complex interactions between atoms or molecules are replaced by simple transition rules on a lattice that abstract the essence of these interactions. The appeal of such models stems from the fact that their rules can be easily implemented in efficient kinetic Monte Carlo (KMC) algorithms. This enables a comprehensive analysis of their statistical characteristics, which can be compared directly with experiments [4–6].

A complementary approach is based on postulating a stochastic differential equation. Solutions of such equations typically focus on the asymptotic kinetic roughening regime, where the standard deviation $W(L,t)$ of the surface profile exhibits dynamic scaling [7]:

$$W(L,t) = [\langle h^2\rangle - \langle h\rangle^2]^{1/2} \sim L^\alpha f(t/L^z)\,. \qquad (1)$$

Here, $h(\mathbf{x},t)$ is the surface height at position $\mathbf{x}$ and time t, L is the lateral viewing scale, α is the roughness exponent, z is the dynamic exponent, and f is a scaling function. At early times ($t \ll L^z$), $f(x) \sim x^\beta$ and $W \sim t^\beta$, where β is the growth exponent and $z = \alpha/\beta$. For long times ($t \gg L^z$) $f \to$ constant, so the saturated roughness $W_{\rm sat} \sim L^\alpha$. The connection to a lattice model is based on comparing exponents and invoking universality [2].

The foregoing paradigm can be justified for many models [2, 8], but outstanding issues persist in some cases, most notably, ballistic deposition (BD). Originally formulated as a model for aggregation and sedimentation [9, 10], BD is the prototypical model of nonconserved growth, in which the volume of material over the substrate is not equal to that deposited, in this case because of void formation. In classic BD [9, 10] a particle impinges on a randomly chosen lattice site and irreversibly attaches to the first vertical or lateral nearest neighbor encountered. The updating algorithm for the integer heights $h_i(n)$ at site i after n depositions is

$$h_i(n+1) = \max\left(h_{i-1}(n), h_i(n)+1, h_{i+1}(n)\right)\,, \qquad (2)$$

for $i = 1, 2, \ldots, L$, where $\max(x,y,z)$ yields the maximum of the three arguments.

The continuum formulation of BD is thought to be the Kardar-Parisi-Zhang (KPZ) equation [11],

$$\frac{\partial u}{\partial t} = \nu\nabla^2 u + \lambda(\nabla u)^2 + \xi\,, \qquad (3)$$

where $u(\mathbf{x},t)$ is the deviation of the height from its mean at position $\mathbf{x}$ and time t on a d-dimensional surface, ν is the surface tension, λ is the "excess velocity," and ξ is a Gaussian noise with mean zero and covariance

$$\langle \xi(\mathbf{x},t)\,\xi(\mathbf{x}',t')\rangle = 2D\delta(\mathbf{x}-\mathbf{x}')\delta(t-t')\,. \qquad (4)$$

Although among the first surface growth models to be studied with KMC simulations [7], discrepancies remain between the scaling properties of BD and the KPZ equation [12–14], even on one-dimensional (1D) surfaces. Their relationship is even less certain in higher dimensions [15–27], including the suggestion [28] that the two models belong to different universality classes.

In this paper, we report the results of extensive KMC simulations of BD on 1D lattices with up to 2^{20} sites, well beyond the onset of saturation, for up to 10^6 independent realizations. In view of the pitfalls associated with hidden correlations in random number generators [29], which may be especially acute for BD [13], we have used the Mersenne Twister MT19937 [30, 31]. This pseudorandom number generator has a period of $2^{19937}-1$, output that is uniformly distributed in 623 dimensions, implying negligible serial correlation, and has passed the most stringent statistical tests [32]. These properties, and its computational efficiency, make the Mersenne Twister eminently suitable for large-scale KMC simulations.

The massive computational resources required for the simulations reported here relied upon unconventional "overnight office computing." Social networking skills were employed in the development of the Simulation through Social Networking (STSN) project, in which 120-130 computers were utilized for some nine months to drive the KMC simulations of even the largest lattices deep into the saturation region [33]. Details may be found in Refs. [34, 35].

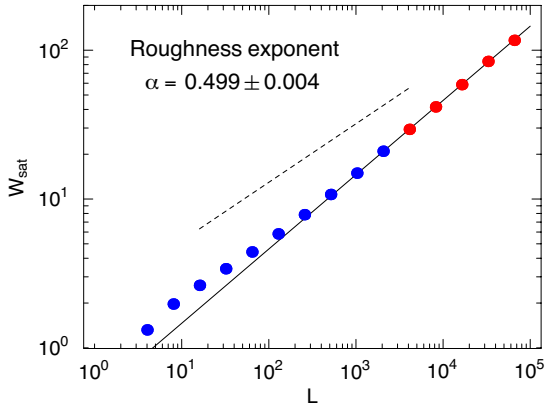

FIG. 1: (Color online) Log-log plot of $W_{\rm sat}$ against L for the data in Table I. Error bars are of the order of the symbol size or smaller. The slope $\alpha = 0.499 \pm 0.004$ of a linear fit to the data points for $L = 2^{12}$–2^{16} (red dots) is in excellent agreement with the KPZ value of $\frac{1}{2}$. The broken line indicates the approximate range of system sizes used in previous work ($L = 2^4$–2^{12}) for calculating α and the resulting slope.

Figure 1 shows a log-log plot of $W_{\rm sat}$ against L using the data in Table I. $W_{\rm sat}$ was calculated by taking samples every 4τ to τ monolayers (ML), depending on the lattice size, where $\tau \sim L^{3/2}$ is the relaxation time [38], to ensure that the data points were statistically independent, and taking binned horizontal averages to alleviate any drift in the data over time [2, 39]. Simulations for $L = 16,384$, $L = 32,768$, and $L = 65,536$ were carried out for up to 33.5×10^6 layers, but many data points were excluded because of the stretched exponential tail in $W_{\rm sat}$. Stretched exponential tails have also been observed in the dynamical structure factor in the stationary regime of the $1+1$-dimensional KPZ equation [40, 42].

Most apparent from Fig. 1 is that an accurate estimate of α requires system sizes beyond $L = 2^{11}$ because of the slow approach to asymptotic scaling. For the smallest systems there is appreciable deviation from the asymptotic behavior because of finite-size effects which persist even to system sizes of 2^{11}. Our estimate of

$$\alpha = 0.499 \pm 0.004\,, \tag{5}$$

obtained from the fit between $L = 2^{12}$ and $L = 2^{16}$, captures the value of $\alpha = \frac{1}{2}$ for the 1D KPZ equation [11]. To our knowledge, this is the first time that the roughness exponent of BD has been shown to agree with the KPZ value (within the error bounds) directly from an analysis of simulation data and without invoking any scaling corrections [2, 14, 28]. To put our results into perspective, the line from $L = 2^4$ to $L = 2^{12}$ in Fig. 1 indicates the approximate range and slope of the simulation data used in previous work for calculating α, resulting in an appreciable underestimate of this exponent.

The slow approach of α to its asymptotic value suggests that a similar trend should be expected for β. However, in contrast to the calculation of α, which requires simulations that extend well into the saturation regime to obtain accurate values of $W_{\rm sat}$, the problem in determining β is not computational overhead *per se*. Rather, the difficulty lies in precisely delineating the limits of the growth region [14] over which $W \sim t^\beta$.

TABLE I: The saturated roughness $W_{\rm sat}$ of 1D lattice sizes $L = 2^n$ for $n = 2, 3, \ldots, 16$ obtained from KMC simulations with the indicated number of independent realizations. The time $t_\times$ to saturation is $t_\times$ and t_s indicates how far the simulations were continued into the saturation regime. Where none is indicated, the calculated error is smaller than 10^{-2}.

L	$W_{\rm sat}$	Error	Realizations	$t_\times$ (ML)	t_s (10^6 ML)
4	1.33	–	100,000	–	4
8	1.97	–	100,000	–	1
16	2.63	–	93,000	–	1
32	3.40	–	100,000	19.75	1
64	4.41	–	10,000	44.5	1
128	5.82	–	10,000	108	1
256	7.85	–	10,000	259	1
512	10.73	–	10,000	675	1
1,024	14.93	–	7,486	1900	1
2,048	20.95	0.03	1,010	5200	4.1
4,096	29.39	0.05	841	13700	4.1
8,192	41.58	0.1	253	38000	4.1
16,384	58.69	0.2	724	106500	10
32,768	84.09	0.2	407	297000	10
65,536	116.55	1.0	249	770000	10

The growth times t_g and the corresponding β_L are compiled in Table II. The most striking trend in these data is the slow approach to the asymptotic value $\beta = \frac{1}{3}$ [11], which is even more pronounced than that in Fig. 1. Lattice sizes in excess of 2^{18} are needed to obtain β_L to within 1% of the exact value. These observations can be quantified by fitting the data to the scaling form [14]

$$\beta_L = \beta + \frac{A}{L^\lambda}\,. \tag{6}$$

The data in Table II yield (Fig. 2) $A = -0.530 \pm 0.128$, $\lambda = 0.324 \pm 0.043$, and

$$\beta = 0.336 \pm 0.004 \tag{7}$$

for $L = 2^{10}$–2^{17}. The data for the largest lattices were excluded from this fitting because of insufficient accuracy, but the best fit still lies within their error bars.

In measuring t_g, we have expanded the criteria suggested by Reis [14] by using floating "beginning" and "end" points for each lattice size and imposing a maximum time. Figure 3 shows a log-log plot of t_g against L with a linear fit of the data points from $L = 2^{16}$ to $L = 2^{20}$. Only when the slope of this line, which we call the "growth-time exponent" γ, reaches unity can we say that the systems have reached the asymptotic regime. The power-law growth regime is bounded by (i) the (largely L-independent) transient regime, during which the system first follows random deposition, before the BD rules determine the growth characteristics,

TABLE II: The growth exponent β_L and the associated error for lattice sizes $L = 2^n$, with $n = 5, \ldots, 20$ obtained from KMC simulations with the indicated number of realizations. The corresponding growth time t_g over which each β_L is calculated, and its error, are also shown.

L	β_L	Error	Realizations	t_g (ML)	Error
32	0.176	0.01	1,000,000	2	1
64	0.20	0.02	1,000,000	4	5
128	0.224	0.006	1,000,000	10	5
256	0.254	0.002	1,000,000	20	5
512	0.270	0.002	1,000,000	80	10
1,024	0.280	0.002	100,000	284	10
2,048	0.2907	0.001	100,000	700	10
4,096	0.302	0.001	100,000	1,400	100
8,192	0.308	0.001	54,000	4,200	500
16,384	0.312	0.002	810	7,936	1,000
32,768	0.317	0.002	407	23,000	7,000
65,536	0.322	0.0005	800	61,000	4,000
131,072	0.325	0.002	105	130,000	10,000
262,144	0.323	0.01	9	260,000	50,000
524,288	0.334	0.005	2	520,000	100,000
1,048,576	0.332	0.005	2	1,040,000	200,000

and (ii) the approach to the saturation regime, which is strongly L-dependent and corresponds to a deviation from power-law behaviour of the surface width. For small system sizes, the transient and saturation regimes are sufficiently close together that the growth exponent deviates significantly from the asymptotic BD value (inset to Fig. 3). But, as L increases, the time between the transient and saturation regimes increases and eventually become sufficiently separated to enable true BD behaviour to develop. It is for these values of L that we observe the slope of unity in Fig. 3.

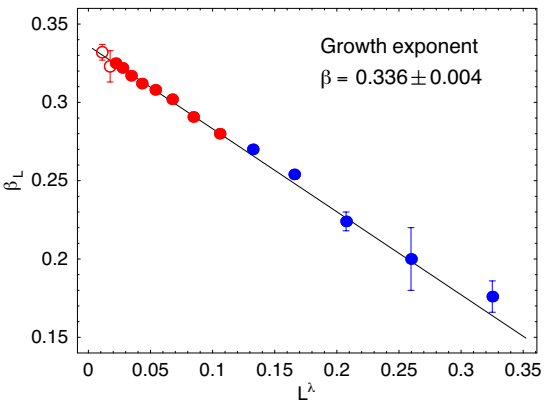

FIG. 2: (Color online) Effective growth exponents β_L plotted against L^λ for the data in Table II with optimized parameters in the scaling form (6). System sizes $L = 2^{10}$–2^{17} (red points) were used in the fit, with smaller lattices (blue points) having growth regions that are too short to give reliable results. System sizes $L = 2^{18}$ and $L = 2^{20}$ (red circles) were excluded from the fit because of insufficient accuracy. The data point corresponding to $L = 2^{19}$ has been omitted for clarity.

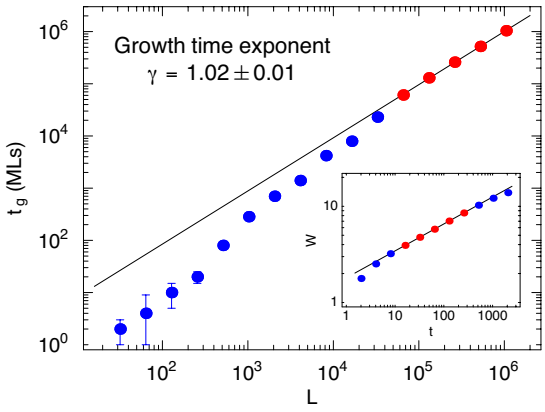

FIG. 3: (Color online) Log-log plot of t_g against L for the data in Table II. The slope $\gamma = 1.02 \pm 0.01$ of a linear fit to the data points from $L = 2^{16}$–2^{20} (red dots) approaches unity, indicating the onset of the asymptotic regime. Inset: Log-log plot of W against t for $L = 1024$, showing the transient regime and approach to saturation (blue dots) bounding the growth regime (red dots and gray shading). The slope of the linear fit within the growth regime is $\beta_L = 0.280 \pm 0.002$.

The scaling relation (1) implies that plots of W/L^α against t/L^z for different system sizes "collapse" onto the universal scaling function f. Our estimate of $z = \alpha/\beta$ from the values of α in (5) and β in (6) is $z = 1.485 \pm 0.03$ [41]. The KPZ value of $z = \frac{3}{2}$ lies within the uncertainty of this estimate. Figure 4 shows the data collapse for $L = 2^{14}, 2^{15}, 2^{16}$. The values of α for these sizes are well into the asymptotic regime (Fig. 1) and the corresponding values of β are within $\sim$0.01 of the asymptotic value of $\beta = \frac{1}{3}$ (Table II). We have used our best estimates of $\alpha = 0.499$ and $\beta = 0.336$ in this plot, but there are few discernible differences if the exact values are used instead.

The high quality of this data collapse, which is indica-

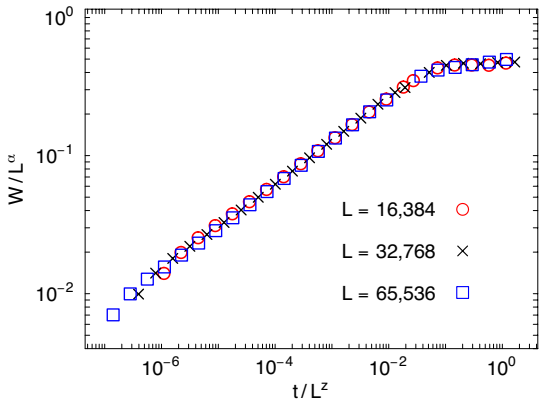

FIG. 4: (Color online) Data collapse for the roughness for sizes $L = 16,384$, $L = 32,768$, and $L = 65,536$ with $\alpha = 0.499$ and $z = 1.485$ determined directly from our simulations. The data points for each lattice size were taken at times $t = 2^k$.

tive both of the accuracy of our data and the fact that these systems lie within the asymptotic scaling regime, invites a comparison with the scaling function of the KPZ model [43]. However, the disparity in the roughness of the surfaces produced by the two models means that the scaling functions are different. This does not preclude the 1D BD model and KPZ equations from belonging to the same universality class, but casts further doubt [28] on the KPZ equation as the continuum expression of BD.

To summarize, we have used massive KMC simulations of BD onto 1D surfaces to demonstrate the slow approach of this system to the asymptotic scaling regime. The exponents α and β were shown to converge to the exact values obtained from the KPZ equation, with systems of up to 2^{20} sites required for a clear indication of convergence. We have used only a single random generator, the Mersenne Twister MT19937, so our results shed no light on the reason for the slow convergence. However, given the long period of this random number generator and its other statistical and operational properties, this is likely an intrinsic property of BD. Future work on 1+1-dimensional BD will focus on more detailed comparisons between our simulations and numerical solutions of the KPZ equation [42, 43].

We conclude with a few remarks about the implications of our results for simulations of BD in higher dimensions. Preliminary simulations on two-dimensional substrates suggest that the slow convergence toward asymptotic scaling persists for higher dimensional substrates, but we have not yet determined the rate of convergence. In this regard, a plot such as Fig. 3 is vital for indicating if a particular system size exhibits statistical characteristics of the asymptotic scaling regime. This will be taken up in a future publication.

BF would like to express his deep gratitude to IASBS staff and students for making the STSN project possible. He would also like to thank S. N. Rasuli and especially M. R. Kolahchi for thoughtful discussions.

[1] T. Halpin-Healy and Y.-C. Zhang, Phys. Rep. **254**, 215 (1995).
[2] A.-L. Barabási and H. E. Stanley, *Fractal Concepts in Surface Growth* (Cambridge University Press, Cambridge, 1995).
[3] A. Pimpinelli and J. Villain, *Physics of Crystal Growth* (Cambridge University Press, Cambridge, 1999).
[4] T. Shitara *et al.*, *Phys. Rev. B* **46**, 6815 (1992).
[5] C. Ratsch *et al.*, Surf. Sci. **329**, L599 (1995).
[6] J. W. Evans, P. A. Thiel and M. C. Bartelt, Surf. Sci. Rep. **61**, 1 (2006).
[7] F. Family and T. Vicsek, J. Phys. A. **18**, L75 (1985).
[8] C. A. Haselwandter and D. D. Vvedensky, Phys. Rev. E **77**, 061129 (2008).
[9] M. J. Vold, J. Colloid Interface Sci. **18**, 684 (1963).
[10] D. N. Sutherland, J. Colloid Interface Sci. **22**, 300 (1966).
[11] M. Kardar, G. Parisi, and Y.-C. Zhang, Phys. Rev. Lett. **56**, 889 (1986).
[12] R. M. D'Souza, Int. J. Mod. Phys. C **8**, 941 (1997).
[13] R. M. D'Souza, Y. Bar-Yam, and M. Kardar, Phys. Rev. E **57**, 5044 (1998).
[14] F. D. A. Aarão Reis, Phys. Rev. E **63**, 056116 (2001).
[15] M. Schwartz and S. F. Edwards, Europhys. Lett. **20**, 310 (1992).
[16] J. P. Bouchaud and M. E. Cates, Phys. Rev. E **47**, R1455 (1993).
[17] J. P. Doherty *et al.*, Phys. Rev. Lett. **72**, 2041 (1994).
[18] Y. Tu, Phys. Rev. Lett. **73**, 3109 (1994).
[19] M. A. Moore *et al.*, Phys. Rev. Lett. **74**, 4257 (1995).
[20] T. Blum and A. J. McKane, Phys. Rev. E **52**, 4741 (1995).
[21] M. Lässig and H. Kinzelbach, Phys. Rev. Lett. **78**, 903 (1997).
[22] J. K. Bhattacharjee, J. Phys. A **31**, L93 (1998).
[23] M. Lässig, Phys. Rev. Lett. **80**, 2366 (1998).
[24] C. Castellano, M. Marsili, and L. Pietronero, Phys. Rev. Lett. **80**, 3527 (1998).
[25] E. Marinari, A. Pagnani, and G. Parisi, J. Phys. A: Math. Gen. **33**, 8181 (2000).
[26] F. Colaiori and M. A. Moore, Phys. Rev. Lett. **86**, 3946 (2001).
[27] F. D. A. Aarão Reis, Phys. Rev. E **69**, 021610 (2004).
[28] E. Katzav and M. Schwartz, Phys. Rev. E **70**, 061608 (2004).
[29] A. M. Ferrenberg, D. P. Landau, and Y. J. Wong, Phys. Rev. Lett. **69**, 3382 (1992).
[30] M. Matsumoto and Y. Kurita, ACM Trans. Model. Comput. Simul. **2**, 179 (1992).
[31] M. Matsumoto and T. Nishimura, ACM Trans. Model. Comput. Simul. **8**, 3 (1998).
[32] P. L'Ecuyer and R. Simard, ACM Trans. Math. Softw. **33**, art. 22 (August 2007).
[33] Social computing is not a new concept. "Volunteer computing" started in the mid-1990s [36] and, by the end of that decade, expanded into the now well-known @home projects in which many thousands of personal computers work together on a single task [37]. STSN is a combination of volunteer and grid computing.
[34] `http://www.iasbs.ac.ir/els/farnudi`.
[35] B. Farnudi, *Scaling and Universality in Deposition Models of Growth*, PhD thesis, (University of London, 2010, unpublished). Available online at: `http://www.imperial.ac.uk/research/cmth/research/theses/`.
[36] D. Anderson, ACM Queue **3**(6), 18 (2005).
[37] Berkeley Open Infrastructure for Network Computing: `http://boinc.berkeley.edu`.
[38] F. D. A. Aarão Reis, Physica A **316**, 250 (2002).
[39] F. D. A. Aarão Reis, private communication.
[40] V. G. Miranda and F. D. A.Aarão Reis, Phys. Rev. E. **77**, 031134 (2008).
[41] In fact, we may be able to calculate z from the stationary structure factor, independently of α and β, as described in Ref. [42] for the KPZ equation.
[42] E. Katzav and M. Schwartz, Phys. Rev. E **69**, 052603 (2004).
[43] K. Ma and C. B. Yang, Mod. Phys. Lett. B **20**, 697 (2006).